Published in final edited form as:
Exp Neurol. 2013 February ; 240: 44–56. doi:10.1016/j.expneurol.2012.11.007.

Expression of human E46K-mutated α-synuclein in BAC-transgenic rats replicates *early-stage* Parkinson's disease features and enhances vulnerability to mitochondrial impairment

Jason R. Cannon[1,2,*], **Kindiya D. Geghman**[3,*], **Victor Tapias**[2,*], **Thomas Sew**[2], **Michelle K. Dail**[2,4], **Chenjian Li**[5,#], and **J. Timothy Greenamyre**[2,#]

[1]School of Health Sciences, Purdue University, West Lafayette, IN 47907

[2]Pittsburgh Institute for Neurodegenerative Diseases, University of Pittsburgh, Pittsburgh, PA 15260

[3]Weil Medical College, Cornell University, New York, NY 10065

[4]Medical Scientist Training Program, University of Pittsburgh School of Medicine, Pittsburgh, PA 15260

[5]Department of Neurology, Mount Sinai School of Medicine, New York, NY 10029

Abstract

Parkinson's disease (PD), the second most common neurodegenerative disorder, is etiologically heterogeneous, with most cases thought to arise from a combination of environmental factors and genetic predisposition; about 10% of cases are caused by single gene mutations. While neurotoxin models replicate many of the key behavioral and neurological features, they often have limited relevance to human exposures. Genetic models replicate known disease-causing mutations, but are mostly unsuccessful in reproducing major features of PD. In this study, we created a BAC (bacterial artificial chromosome) transgenic rat model of PD expressing the E46K mutation of α-synuclein, which is pathogenic in humans. The mutant protein was expressed at levels ~2–3-fold above endogenous α-synuclein levels. At 12 months of age, there was no overt damage to the nigrostriatal dopamine system; however, (i) alterations in striatal neurotransmitter metabolism, (ii) accumulation and aggregation of α-synuclein in nigral dopamine neurons, and (iii) evidence of oxidative stress suggest this model replicates several preclinical features of PD. Further, when these animals were exposed to rotenone, a mitochondrial toxin linked to PD, they showed heightened sensitivity, indicating that α-synuclein expression modulates the vulnerability to mitochondrial impairment. We conclude that these animals are well-suited to examination of gene-environment interactions that are relevant to PD.

[#]Corresponding authors: J. Timothy Greenamyre, M.D., Ph.D., Pittsburgh Institute for Neurodegenerative Diseases, University of Pittsburgh, 3501 Fifth Avenue, Suite 7039, Pittsburgh, PA 15260, Tel: 412-648-9793, Fax: 412-648-9766, jgreena@pitt.edu, Chenjian Li, Ph.D., Friedman Brain Institute, Mount Sinai School of Medicine, NYU, One Gustave L. Levy Place, Box 1137, Annenberg Bldg, Rm 20-72, New York, NY 10029, (O) 212-241-1705, chenjian.li@mssm.edu.
[*]The authors wish it to be known, that in their opinion, the first three authors should be regarded as joint First Authors.

Keywords

Parkinson's disease; alpha-synuclein; BAC-transgenic; E46K; rotenone

Introduction

Parkinson’s disease (PD) is a common, age-related, progressive neurodegenerative disorder. Clinical diagnosis is based on behavioral criteria, and requires the presence of bradykinesia and at least one additional feature: resting tremor, rigidity or postural imbalance (Litvan, et al., 2003). Pathologically, the disease is characterized by progressive loss of nigral dopamine neurons and their projections, which results in striatal dopamine depletion and accounts for many of the motor symptoms (Cannon and Greenamyre, 2010). A second pathological hallmark of the disease is the presence of Lewy bodies in nigral dopamine neurons (Forno, 1996), which are composed, in part, of the protein α-synuclein (Spillantini, et al., 1997). The presence of α-synuclein in Lewy bodies, together with the fact that mutations in the gene encoding α-synuclein cause rare genetic forms of PD (Polymeropoulos, et al., 1997), suggests a pathogenic role for the protein in both sporadic and genetic forms of the disease.

About 10% of PD cases are caused by single gene mutations; the remainder are termed ‘sporadic’ or ‘idiopathic’. Although most of these cases are thought to arise from a combination of environmental factors and genetic predisposition, the nature and mechanisms of such interactions in pathogenesis are poorly understood, and there are few relevant animal models. Genetic mammalian models of PD have been largely comprised of knockout mice, and more recently rats that mimic a loss-of function gene or transgenic mice that express a disease causing mutation. Unfortunately, genetic models utilizing rare disease-causing mutations in α-synuclein, Parkin, Pink1, and DJ-1 have mostly failed to recapitulate the key features of human PD (Chandran, et al., 2008, Goldberg, et al., 2003, Goldberg, et al., 2005, Itier, et al., 2003, Kitada, et al., 2007, Manning-Bog, et al., 2007, Masliah, et al., 2000, Perez, et al., 2005, Richfield, et al., 2002, Von Coelln, et al., 2004, Yamaguchi and Shen, 2007). Moreover, the predictive value of current models for testing disease-modifying therapies remains uncertain. Thus, additional and improved models are required.

Current genetic rat models have typically utilized viral vector-based approaches that require intracerebral infusion (Welchko, et al., 2012), a surgical procedure that does not transduce all relevant neurons and does not elicit effects throughout the entire lifespan. Bacterial artificial chromosomal (BAC) technology has allowed for the production of transgenic rodents with over-expression levels much closer to physiological levels (~2–5 fold). BACs contain large genomic DNA sequences (typically 200 kb with a capacity of up to 700 kb) that carry all the native genomic structures including promoters and regulatory elements of a gene (Shizuya, et al., 1992, Yang and Gong, 2005). As α-synuclein has four isoforms that are differentially expressed throughout the brain (McLean, et al., 2012), creating a BAC-α-synuclein transgenic rodent ensures more accurate spatio-temporal protein expression compared with using traditional cDNA. For many PD studies, rats offer significant advantages over mice, particularly for behavioral assessment, neuroanatomical comparisons to humans, and the ability to analyze more endpoints because of tissue availability (Whishaw and Kolb, 2004).

To date, three different α-synuclein point mutations have been identified to cause PD in an autosomal dominant manner. The E46K mutation is the most recently identified of the three, and patients with the mutation have a typical motor and pathological PD phenotype (Zarranz, et al., 2004). Further, functional studies have shown that the mutation promotes

protein aggregation (Choi, et al., 2004). Recently, an E46K mouse line using the prion-promoter was developed and shown to exhibit late-life behavioral deficits and α-synuclein inclusion formation (Emmer, et al., 2011). However, in this report, aggregation did not appear to occur in nigral dopamine neurons as it does in human PD, and striatal dopamine levels and nigral dopamine counts were not reported.

The goals of the current study were to: (i) create a BAC-transgenic rat model expressing E46K-mutated α-synuclein, (ii) characterize the neurochemical and histological effects of E46K-mutated α-synuclein expression, and (iii) test whether these animals exhibit heightened sensitivity to rotenone, a mitochondrial toxin that has been identified as a risk factor for human PD (Betarbet, et al., 2000, Tanner, et al., 2011).

Materials and Methods

Supplies and Animals

All supplies were obtained from Sigma-Aldrich, Co. (St Louis, MO, USA), unless otherwise noted. All experiments described below involving the creation and characterization of this new transgenic animal model were approved by the Institutional Animal Care and Use Committees at Cornell University and the University of Pittsburgh.

Transgenic rat design

Transgenic rats expressing E46K mutated α-synuclein were created using bacterial artificial chromosomal technology as described below.

The α-synuclein BAC—A human wild-type α-synunclein BAC (wtBAC) containing chloramphenicol (chl) resistance (Caltech, # 2026 H24) was modified to create an α-synuclein mutant with the human E46K point mutation. These mutations were engineered using techniques pioneered and previously described by Gong and colleagues (Gong, et al., 2002).

Site modification—Staggered PCR was used to create mutations surrounded by 'A box' and 'B box' homology arms, each of 500–700bp in length (Figure 1). Mis-sense and silent point mutations were designed around the intended region to create the disease mutation, and (a novel restriction site for easy gene identification. The E46K product contains a NcoI (C/CATGG) restriction site. Primers carrying these mutations at their 5' ends consisted of the internal set of primers for the AB box products. The 5' end of the A Box Forward primer contained an AscI (GG/CGCGCC) restriction site and 5' end of the B Box Reverse primer contained a PacI (TTAAT/TAA) restriction site. It is important to note that none of these restriction sites are found anywhere in the AB box in the unmodified gene. Table 1.1 details the primers designed for these experiments.

The pLD53 vector insertion—The mutated 'AB box' was cloned into a pLD53 vector within its AscI/PacI sites (Metcalf, et al., 1996). The pLD53 vector contained an ampicillin (amp) resistance gene, a SacB gene that confers toxicity and death to sucrose exposed cells, an R6kγ origin of replication site, and a RecA protein to support homologous recombination. The ligated vector was transformed into Pir2 cells (Invitrogen), which produce the π protein essential for R6kγ replication.

BAC cointegration—The AB box containing pLD53 vector was electroporated into human α-synuclein BAC expression *E. coli* cells. Vectors that integrated into the BAC via homologous recombination were selected for through serial dilutions with increased amp concentrations, and then grown on chl and amp resistance plates. Promising candidates were

identified through enzymatic digestion, with ApaLI & XbaI for the A53T mutation and NcoI for the E46K mutation. Successful cointegration was confirmed through Southern hybridization using a probe to the A box.

BAC resolution—To homologously recombine out the vector, cells were plated on sucrose allowing the SacB negative selection marker to excise pLD53. Colonies that underwent pLD53 excision and contained the novel mutation (half of the recombinations resulted in a return to the original α-synuclein wtBAC) were then identified through a second Southern hybridization using a probe to the A box.

BAC sequencing and linearization—All six exons and surrounding intronic regions were sequenced to confirm that no unwanted mutations were present (Table 1.2). The 5' BAC end was sequenced using the built-in T7 primer sequence to identify exact contents of the BAC. This verification had been carried out previously in the LRRK2-G2019S and LRRK2-R1441G lines.

For all five BACs, vectors were removed through digestion and Sepharose bead columns. To determine concentration and DNA integrity, a sample of the linearized BAC was run in a pulse field gel. BACs were sent to Dr. Thomas Saunder's lab at the University of Michigan for pronuclear injection in Sprague Dawley rat embryos (Filipiak and Saunders, 2006). Founders were identified through tail genotyping and shipped to our facility.

Transgenic animal production—DNA was injected into fertilized eggs at the single-cell stage, and these pronuclei were transplanted into pseudopregnant female surrogate rats. Resultant offspring were genotyped to identify pups that expressed the transgene.

Genotyping—Rat pup tail tips were incubated at 55°C for 2.5 h in lysis buffer (25 mM NaOH, 0.2 mM EDTA, 1.5 μg/μL), boiled at 95°C for 20 min, and immediately put on ice for 2 min. An equal concentration of neutralization buffer (40 mM TRIS HCl, pH 7.4) was added and the sample was spun down at top speed for 2 min. Two μL of supernatant were added to the PCR reaction. Primers to Exon 1 were used.

Identification of high expresser rat lines—For our experiments, we aimed to identify the founders that transmitted the transgene and produced offspring that had high levels of human α-synuclein expression in the brain. At 6–7 weeks of age (unless otherwise indicated), brain lysates of TG F1 pups and their littermate controls were analyzed for α-synuclein expression via western blot.

SDS-PAGE western blot—As anesthetics are known to affect DA release and brain chemistry, awake animals were quickly sacrificed via guillotine without anesthetic. Brains were extracted and, in some cases, dissected into specific regions. For regional expression, areas obtained were: the olfactory bulb, frontal cortex, striatum, ventral midbrain (includes the SNpc), cerebellum, and spinal cord. Brains were homogenized using RIPA buffer (50 mM Tris, pH 8.0, 150 mM NaCl, 5 mM EDTA, 1% NP40, 0.5% sodium deoxycholate, 0.1% SDS) containing 1X protease inhibitor cocktail (Roche). After centrifugation at 14,000 g for 15 min, lysates (the supernatant) were collected and protein concentrations were measured using DC protein assay (Bio-Rad). Thirty μg of each sample was boiled, separated on either a 12% or a 4–12% gradient polyacrylamide gel with MOPS SDS running buffer, and transferred to a PVDF membrane (Millipore). Membranes were probed with α-synuclein antibody (sc7011R, Santa Cruz, 1:1000), human specific α-synuclein antibody (LB509, Abcam, 1:1000), and an anti-actin control (MAB1501, Millipore, 1:6000). For westerns developed on film, a 5% milk in TBST blocking solution was followed by 1% milk in TBST

for primary and secondary HRP-conjugated antibodies. Signal detection with enhanced chemiluminescence (Pierce) was used to visualize our results on exposed film. To determine expression levels, results were quantified with ImageJ software.

Fluorescent In-Situ Hybridization mapping of BAC integration

Fibroblasts: Rat tail tips were sterilized and biopsied. Tips were diced to <0.5 mm and incubated in high-glucose DMEM with 20% heat-inactivated fetal bovine serum (FBS), 1000U/mL collagenase type II, antibiotics (100U/ml penicillin and 100 μg/ml streptomycin), and 0.25 μg/mL fungizone overnight at 37°C with 5% CO_2. Cells were then dislodged by repeated pipetting, passed through sterile nylon netting and centrifuged 5 min at 200 *g*. The pellet was resuspended in DMEM with 20% FBS, antibiotics and fungizone, and seeded until 70–80% confluent.

Metaphase harvest of rat cell lines: Prior to harvesting, 70–80% confluent cultures were treated with 0.05 ug/mL Colcemid (Karyomax, Invitrogen) for 60–90 minutes, according to standard cytogenetics procedures. Cells were trypsinized to a single cell suspension, pelleted at 180 g for 8 min and resuspended in warm 0.075 M KCl. After 8 min incubation at 37°C, the hypotonic solution was diluted with approximately 1/4 volume of 3:1 methanol/glacial acetic acid fixative, gently mixed, and the cells pelleted as before. The supernatant was removed and the cell pellet loosened by gently flicking the base of the tube. The cells were then fixed in three changes of fixative. Fixed cell suspensions were stored at −20°C.

Fixed metaphase preparations were dropped onto dry slides and the quality of spreading assessed by phase microscopy. Spreading was adjusted by altering the drying time, increasing local humidity (water bath) or applying heat (hotplate). Slides were then air-dried and aged (37°C for 1–2 days, or 60°C for several hours).

Fluorescent In-Situ Hybridization: One μg of human BAC DNA was labeled by nick translation with Red dUTP (Enzo, Abbott Molecular), ethanol precipitated, and resuspended in 10 μL TE buffer. Following resuspension, 1 μL of labeled probe was mixed with 14 μL hybridization buffer (50% formamide, 2× SSC, 10% dextran sulfate, 0.1% SDS, 1×Denhardt's solution, 40 mM sodium phosphate buffer, pH=7) and applied to a warm slide on a warming bench, then covered with a 22 × 32 mm coverslip. Coverslip were sealed in place with rubber cement and the slides were denatured at 70°C for 2 min with a HYBrite automated hybridizing station (Abbott Molecular). The slides were then transferred to a 37°C incubator and hybridized overnight. A control slide of normal human male metaphase spreads was included.

Following hybridization, the rubber cement was removed and the coverslips soaked off in 2× SSC/0.1% Igepal CA 630 at room temperature. The slides were then incubated in 0.4× SSC/0.3% Igepal at 73°C for 2 min, washed in 2× SSC/0/1% NP-40 at room temperature, then rinsed in 2× SSC. After staining in 0.08 μg/mL DAPI in 2× SSC for 2–3 min, slides were quickly rinsed twice in distilled water and air dried. They were then mounted in antifade solution (Vectashield, Vector labs) and stored in boxes at 4–8°C, ready for analysis.

Slides were scanned using a Zeiss Axioplan2ie epifluorescence microscope equipped with a digital imaging system (MetaSystems Group, Inc.). Metaphase images were captured and the DAPI-stained chromosomes were inverted to resemble conventional G-banding and karyotyped to identify the location of the FISH signals. A minimum of 15 metaphases was examined for each sample.

Determination of PD phenotype

At up to 12 months age, no overt bradykinesia, postural instability, or rigidity was observed in either the transgenic or wild-type animals. Thus, animals were evaluated for neurochemical and pathological changes at 12 months of age.

Rats were euthanized by rapid decapitation and the brain was rapidly removed, cooled in ice-cold PBS for ~3 min and then bisected sagittally. Half the brain was used for neurochemical analysis and the other half for histology.

Neurotransmitter analysis—A 2.0 mm coronal brain slice was acquired using a rat brain matrix and the dorsolateral striatum was quickly dissected, flash frozen in liquid nitrogen and processed for determination of dopamine, serotonin, and metabolites by HPLC with electrochemical detection as previously described (Cannon, et al., 2009). The amount of each neurotransmitter was determined by area under the peak and a standard curve generated from the high-purity standards. Neurotransmitter amounts were reported relative to tissue protein, using a Lowry-style protein assay (Lowry, et al., 1951).

Histology—One brain hemisphere was post-fixed in 4% paraformaldehyde for 7 days, changed to 30% sucrose until sinking and then cut at 35 μm on a freezing-stage sliding microtome. The sections were stored in cryprotectant at 4°C until use.

For confocal analysis of α-synuclein accumulation, the sections were washed for 10 min 6 times in PBS and then blocked in 4% normal donkey serum in 0.3% triton x-100 and PBS. The sections were then incubated in the primary antibody solution containing one or more of the following antibodies: mouse anti-α-synuclein (LB509), Ab27766, Abcam, Cambridge, MA, USA, 1:250; sheep anti-α-synuclein, AB5334P, Millipore, Billerica, MA, USA, 1:3000; rabbit anti-tyrosine hydroxylase, AB152, Millipore, 1:2000; or rabbit anti-MAP2, AB5622, Millipore, 1:2000. The primary antibody was diluted in PBS, containing 1% normal donkey serum and 0.3% triton x-100. The sections were then washed 3 times in PBS and incubated in the following secondary antibodies: Alexa Fluor 488 donkey anti-rabbit (A-21206, Invitrogen, Grand Island, NY, USA, 1:500), Cy3 donkey-anti-mouse (Jackson ImmunoResearch, West Grove, PA, USA, 1:500), and Alexa Fluor 647 donkey anti-rabbit (A-31573, Invitrogen, 1:500) for two hours at room temperature. The sections were then washed 3 times in PBS and mounted on glass slide, then cover-slipped, using gelvatol. Immunofluorescence images were acquired using a confocal microscope (FV-1000, Olympus, Center Valley, PA, USA); the acquisition settings were optimized over several sections and the settings at each magnification were maintained throughout acquisition. Any adjustments to intensity, brightness or contrast were made identically to every image in a series at a given magnification.

Dopamine terminal density quantification—Striatal sections (1 in 12) were stained as above, except mouse anti-tyrosine hydroxylase (MAB318, Millipore, 1:2000) was the primary antibody and the secondary was IR800 donkey anti-mouse (926–32212, Licor, Lincoln, NE, 1:500). The sections were then scanned on an Odyssey imager (Licor) and the average tyrosine hydroxylase immunofluorescence in the dorsal striatum was determined over 5–7 sections/animal as previously described (Cannon, et al., 2011).

Nitrotyrosine quantification—Staining was conducted as above, except antigen retrieval using pepsin digest solution (00–3009, Invitrogen) was used 5 min at 37°C (before blocking solution). Double immunofluorescence staining was performed 72 h at 4°C with primary antibodies: sheep anti-tyrosine hydroxylase (Ab1542, Millipore, 1:3000), and rabbit anti-NT (06–284, Millipore, 1:500). For double labeling, the primary antibodies were detected with

Alexa Fluor 488 donkey anti-sheep (A-11015, Invitrogen, 1:500), and Cy3 donkey anti-rabbit (711-165-152, Jackson ImmunoResearch, 1:500). To determine the levels of nitrotyrosine, ~1 in 12 nigral sections were processed for tyrosine hydroxylase and nitrotyrosine immunoreactivity. Nigral images from the brain were acquired using a confocal microscope (Olympus Fluoview 1000) at 40× magnification (N.A. = 0.9). Fluorescent intensity was determined by drawing regions of interest around nigral dopamine neurons (TH^+). The laser and detector settings were adjusted to avoid saturation. A total of 200–300 TH^+ neurons were analyzed from five coronal SN sections correspondent to six different animals per group. Individual neuron intensity values were used to determine whether TH^+ intensity predicted nitrotyrosine intensity.

Rotenone treatment—Adult, male rats (~6 months old) were treated with daily intraperitoneal rotenone at a dose (2.5 mg/kg.day) below that which typically results in overt neurobehavioral abnormalities and toxicity to the nigrostriatal dopamine system (Cannon, et al., 2009). The rotenone solution was prepared and administered as previously described (Cannon, et al., 2009). This model has previously been shown to be useful in assessing potentiation (Tapias, et al., 2010). Animals were treated with rotenone until they developed severe, mobility-limiting combination of bradykinesia, postural instability, or rigidity as previously described (Cannon, et al., 2009).

Quantitative assessment of neuronal number—Double immunofluorescence staining was performed on one in every six coronal sections in the midbrain as described above, except primary antibody incubation was for 72 h at 4°C with the following primary antibodies: sheep anti-tyrosine hydroxylase (Millipore, 1:3000) and mouse anti-MAP2 (Millipore, 1:2000). For double labeling, the primary antibodies were detected with Cy3 donkey anti-sheep (713-165-003, Jackson ImmunoResearch, 1:500), and Alexa Fluor 647 (A-31571, Invitrogen) after incubation for 1 h at RT. Fluorescent images were acquired using an automated Nikon 90i upright widefield microscope using a 20× objective (NA = 0.75), equipped with a linear-encoded motorized stage and Q-imaging Retiga cooled CCD camera. Micrographs were analyzed using the NIS-Elements software and a region of interest was drawn around the substantia nigra. Quantification of neuronal numbers was performed by a single investigator blinded. The software counted all cells in which MAP2 and TH colocalized and that contained H33342-positive nuclei. The method yields virtually identical results to manual stereology, but has a lower coefficient of error (<0.05 for each animal) owing to the much greater number of neurons sampled (unpublished data).

Statistical analysis

All data were analyzed by the Student's *t*-test, except for the survival curve, which was analyzed by a Log-rank test. For all experiments, $p<0.05$ was deemed significant.

Results

Model Creation and Validation

E46K cointegration—The E46K mutation with A and B-box homology arms was successfully integrated into the pLD53 vector. The E46K-pLD53 vector was 8117bp and contained the engineered Nco1 restriction site (bp 0), followed by additional sites at bp 5880 and 6454. Cutting at these sites produced bands of the following sizes: 1660bp (A-box), 5883bp (B-box), and 574bp. The AB box in the wtBAC was 6964bp when cut with Nco1. Figure 1 is a schematic of the vector and wtBAC.

E46K resolution—Resolution had a 50% chance of occurring within the A-box, and 50% within the B-box. Since the vector integrated in the A-box, if resolution occurred through

the A-box the BAC would return to a wtBAC, and resolution through the B box would maintain the mutation. A wtBAC would produce a 6964bp band and an E46K-BAC would produce a 4944bp band when probed with A-box αATP (Figure 1C).

As expected, about half of the bands resolved to produce a successfully mutated E46K-BAC (Supplemental Figure 1). One of the candidates was selected for pronuclear injection.

Sequencing of BACs—There were no unintended mutations in any of the six α-synuclein exons or their surrounding regions. The linearized BAC was ~175kb, and the 5' end was sequenced to determine the regions included in the BAC. The human α-synuclein gene is ~110kbp, and the 2026H24 BAC contains the entire gene, including 30kbp upstream of the 5' end of exon 1 and 35kbp downstream of the 3' end of the exon 6 stop codon. Bioinformatic analysis revealed no additional gene sequences or predicted gene sequences in our BAC.

Transgenic animal production—The total number of Sprague-Dawley pups born was n = 116, the number of TG founders was n = 16, and the success rate of the injections was 13.8%. There appeared to be neither infertility problems nor embryonic lethality as a result of E46K transgene expression. The litter sizes were large and comparable to non-TG animal breeding, and about half of the progeny were TG.

Highest expresser identification—We identified Founder #70 as our highest expresser and Founder #43 as our second highest expresser (Supplemental Figure 2). For the remainder of our experiments, we chose to work with line 70. Line 70 FISH analysis revealed that the E46K BAC integrated into a single site (chromosome 1q34~6) and sequencing re-confirmed the E46K and NcoI mutations (Figure 2).

Regional expression levels—Western blots displaying regional brain expression of α-synuclein in our E46K line 70 demonstrated that the protein was ubiquitously expressed throughout the brain and spinal cord. Total α-synuclein levels followed a relatively consistent pattern between the TG and wild-type littermate controls (Figure 3A), with the cerebellum and spinal cord displaying lower levels of α-synuclein than the frontal cortex and striatum. These results were also consistent in the human-specific α-synuclein westerns (Figure 3B). Thus, the increase in α-synuclein is due to expression of the human transgene, and the transgene expression pattern is similar to the expression pattern of the endogenous protein.

Model characterization

Alpha-synuclein accumulation in E46K transgenic rats—Immunohistochemistry for α-synuclein (Figure 4) shows that in 12-month old transgenic rats there are both diffuse accumulation (low magnification images) that appears to occur in the neuropil (likely in processes) and intracellular accumulation and aggregation (high magnification images). Importantly, while the transgene is expressed diffusely throughout the brain, within the substantia nigra, intracellular α-synuclein accumulation and aggregation are primarily limited to dopaminergic neurons (colocalization with tyrosine hydroxylase positive neurons). Antibodies to both total and human aggregated α-synuclein (LB509) illustrate expression differences between wild-type and transgenic rats. In particular, staining for LB509 is virtually absent in wild-type animals, while intracellular accumulation and aggregation is clearly observed in animals expressing E46K-mutated α-synuclein. While evidence of accumulation in nigral dopamine neurons are clear, the aggregates appear to be much smaller than those that occur in human PD or in the rat rotenone model, potentially modeling the earliest stages of accumulation. Intracellular α-synuclein accumulation also

occurs in the ventral tegmental area (VTA) dopamine neurons (Supplemental Figure 3). In the striatum, alpha-synuclein accumulation appears to be primarily in processes (Supplemental Figure 4) and in the cortex, accumulation also appears to be primarily in processes (Supplemental Figure 5). Thus, intracellular α-synuclein accumulation and aggregation in the brain regions examined is primarily limited to dopaminergic neurons.

Striatal dopamine terminal density—Quantitative assessment of striatal dopamine terminal density did not reveal differences between wild-type and E46K-expressing animals at 12-month old (Figure 5). The absence of major striatal dopamine terminal loss indicates that there is no overt damage to the nigrostriatal dopamine system ($n = 10$ per group).

Alterations in striatal neurotransmitters—Transgenic rats did not exhibit detectable depletion in striatal dopamine (Figure 6). Striatal serotonin levels were also unaltered (Figure 7). However, dopamine metabolites were significantly reduced (Figure 6). 3,4-Dihydroxyphenylacetic acid (DOPAC) was decreased in transgenics by 24% (5.30 ± 0.47 vs. 6.98 ± 0.59 ng/mg protein, transgenic vs. wild-type ± SEM; $p < 0.05$, Student's *t*-test; $n = 10$) and homovanillic acid (HVA) was also reduced by 24% (4.84 ± 0.39 vs. 6.36 ± 0.59; $p < 0.05$). The serotonergic metabolite, 5-hydroxyindole-3-acetic acid (5-HIAA) was also reduced (Figure 7) by 18% (2.26 ± 0.08 vs. 2.76 ± 0.14; $p < 0.01$).

Transmitter turnover was also decreased in transgenic animals. Striatal dopamine turnover [(DOPAC + HVA)/dopamine) was reduced by 20% (0.1002 ± 0.0032 vs. 0.1254 ± 0.0043; $p < 0.0005$), while serotonin turnover (5-HIAA/5-HT) was reduced (Figure 7) by 19% (0.6413 ± 0.0285 vs. 0.7891 ± 0.0374; $p < 0.01$).

An absence of striatal dopamine depletion confirms that there is not a major lesion to the nigrostriatal dopamine system in the transgenic animals. However, expression of E46K-mutated α-synuclein influences both dopaminergic and serotoninergic metabolism.

Oxidative stress in rats expressing E46K-mutated α-synuclein—Nitrotyrosine levels (immunoreactivity) were increased in transgenic rats (Figure 8). Specifically, in nigral dopamine neurons, nitrotyrosine levels (normalized to tyrosine hydroxylase) were increased by 29% (0.3039 ± 0.0193 vs. 0.2360 ± 0.0108, transgenic vs. wild-type ± SEM; $p < 0.05$; $n = 6$). Thus, expression of E46K-mutated α-synuclein increases oxidative stress in nigral dopamine neurons.

Animals expressing E46K-mutated α-synuclein exhibit heightened sensitivity to rotenone

Emergence of PD phenotype—At a rotenone dose below that which typically induces overt toxicity (2.5 mg/kg/day), transgenic rats exhibited heightened behavioral sensitivity (Figure 9) in response to rotenone treatment. The behavioral features of the rotenone model have been extensively characterized. Chronic rotenone treatment in the rat at 3.0 mg/kg/day results in a bilateral lesion to the nigrostriatal dopamine system that produces motor deficits, including postural instability, rigidity, and bradykinesia. These deficits eventually limit mobility and animals are euthanized (Betarbet, et al., 2000, Cannon, et al., 2009). Emergence of this phenotype has been used to assess potentiation in the rotenone model (Tapias, et al., 2010). Here, expression of E46K-mutated α-synuclein in 6 month-old rats increased transgenic animals' sensitivity to low-dose rotenone, with significant differences observed in the time to emergence of the severe PD-phenotype ($p < 0.01$, Log-rank test, $n = 10$).

Loss of striatal dopamine terminals—While expression of E46K-mutated α-synuclein alone did not induce terminal loss (Figure 5), transgenic animals treated with low-dose

rotenone (2.5 mg/kg/day) exhibited decreased dopamine terminal density (Figure 10). Lesions in the dorsolateral striatum were significant in transgenic animals. Quantitative analysis of tyrosine hydroxylase immunoreactivity revealed significant differences between transgenic and wild-type animals (426.7 ± 25.5 vs. 601.8 ± 27.5, mean fluorescence intensity ± SEM; wild-type vs. transgenic; $p < 0.001$; $n = 9–10$). Thus, expression of E46K-mutated potentiates striatal dopamine terminal loss after low-dose rotenone treatment.

Nigral dopamine cell counts—Differences in nigral dopamine neuron numbers (Figure 11) were not observed between 6-month old wild-type animals and transgenics after low-dose rotenone treatment ($n = 6$ per group). Therefore, major cell loss in the transgenics did not likely occur under the conditions tested. Overt potentiation occurred primarily at the level of terminals (Figure 10).

Discussion

Here, we present the development, validation, and characterization of a new transgenic rat model of PD, carrying an E46K mutated α-synuclein BAC. A thorough validation indicated that the desired mutation was achieved in this new animal model without unforeseen genetic events. Protein levels were physiologically relevant and only ~2–3 fold over endogenous expression. This dosage increase approximates a gene triplication, which is found to confer early onset PD in humans (Singleton, et al., 2003). Though there was no evidence of an overt motor phenotype similar to that which occurs in bilateral neurotoxicant models (behavior was not quantitatively assessed), the animals displayed a decrease in dopamine metabolites in the striatum and α-synuclein accumulation and aggregation and oxidative stress in nigral dopamine neurons – thereby reproducing some features of preclinical PD. The early-stage PD phenotype makes these animals useful for examining the earliest mechanisms of dysfunction in PD and ideal for studies investigating gene-environment interactions. In this regard, we also report that these animals exhibit heightened *in vivo* sensitivity to a mitochondrial toxin (rotenone) that has been implicated as a bona fide risk factor for human PD.

While transgenic animals were evaluated at up to 12 months of age, sensitivity to rotenone was evaluated much earlier, to simulate a mid-life exposure. At six months of age, E46K animals are hypersensitive to rotenone, an environmental toxicant that has been well documented to elicit parkinsonism in rats and other organisms, and which has been identified as a risk factor in human PD (Betarbet, et al., 2000, Tanner, et al., 2011). The majority of E46K rats developed a PD phenotype after one week of exposure to rotenone at a dose (2.5 mg/kg) that does not typically cause toxicity in normal animals. Striatal dopamine terminal density in these animals was reduced compared to wild-type animals. Behavioral deficits and terminal loss are typically only observed at higher doses and over longer time frames in wild-type rats (Cannon, et al., 2009). Thus, our model reveals an interesting gene-environment interaction: expression of E46K-mutated α-synuclein confers heightened sensitivity to a known parkinsonism-inducing neurotoxicant. These results suggest that pathogenic forms of α-synuclein may enhance the toxic effects of mitochondrial impairment. Further, the results suggest that for individuals expressing pathogenic forms of the protein, exposure to mitochondrial toxins, such as certain pesticides, may have deleterious effects on age of onset or disease severity.

Differences in nigral dopamine cell counts were not observed between groups, indicating that in the time frame of this experiment, damage to the nigrostriatal track in transgenic animals was limited to the striatal terminals. While we cannot rule out subtle morphological or functional differences in the substantia nigra between groups, this likely is a simple reflection of that fact that rotenone-induced degeneration, which begins in nigrostriatal

terminals, occurred rapidly in the transgenic rats. As such, the animals developed rather abrupt bilateral striatal dopamine depletion with severe parkinsonian symptoms which required euthanasia before there was time for retrograde degeneration to affect nigral neurons. Future studies at lower rotenone doses would be expected to result in slower development of a lesion to the nigrostriatal dopamine system, where loss of nigral dopamine neurons might be detected and behavioral deficits could be quantitatively assessed.

The phenotype in transgenic animals at 12 months is not indicative of a frank lesion of the nigrostriatal dopamine system. It should be noted that in humans the average age of disease onset is in the 6th decade for patients with E46K mutations (Zarranz, et al., 2004). The relatively short life span of the rodent may make it difficult to reach endpoints indicative of 'late-stage' PD. Nevertheless, the animals we have described here clearly exhibit functional alterations in the nigrostriatal tract. Increased intracellular α-synuclein and oxidative stress in nigral dopamine neurons, in the absence of appreciable cell death, likely represent key pathogenic features of early-stage PD (Braak, et al., 2003). Because of a lack of available clinical data, it is difficult to predict how well the alterations in neurotransmitter metabolite levels and turnover observed in this model predict alterations that may occur in prodromal human PD. However, imaging studies have suggested that decreased dopamine release during stereotyped movements can be apparent using PET scans in the early-stage clinical PD (Goerendt, et al., 2003, Strafella, et al., 2005). Additionally, PET scans have shown alterations in dopamine metabolism in presymptomatic mutant gene carriers (Adams, et al., 2005, Nandhagopal, et al., 2008). Reduced dopamine release has also been reported in transgenic mice over-expressing α-synuclein (Yavich, et al., 2005). Further, numerous other knockout (DJ-1, parkin, and pink1) mouse PD models have reported effects on dopaminergic neurotransmission in the absence of overt neurodegeneration (Goldberg, et al., 2003, Goldberg, et al., 2005, Kitada, et al., 2009, Kitada, et al., 2007). It should be noted that in neurotoxicant-based models with major lesions to the nigrostriatal dopamine system, DA turnover is typically increased, likely resulting from compensatory mechanisms after significant dopamine depletion (Cannon, et al., 2009, Schwarting and Huston, 1996). Thus, in transgenic models without an overt lesion to nigral dopamine neurons or major dopamine depletion, altered dopaminergic neurotransmission may be indicative of a potentially important preclinical event. Our data also indicates that an evaluation of these animals past 12 months of age, as late in the life-span as feasible, would be useful to determine if cell death or dopamine depletion eventually occurs.

Here, we also report alterations in serotonin primarily resulting from decreased levels of 5-HIAA, the primary metabolite of serotonin. As with the dopaminergic alterations, it is difficult to predict how well our findings predict alterations in prodromal human PD. However, much recent work shows that serotonergic alterations occur in the earliest stages of PD. The serotonergic raphe nuclei are affected in the earliest stages of PD, prior to observable pathology in the substantia nigra (Braak, et al., 2003, Braak, et al., 2004). A decrease in SERT binding in the orbitofrontal cortex, caudate-putamen and midbrain has also been found in early stage PD patients (Guttman, et al., 2007). Recent PET data also correlates depression, tremor, weight fluctuations and visual problems in PD patients with in the serotonin transporter and serotonin receptors (Politis and Loane, 2011, Smith, et al., 2012). Effects on serotoninergic neurotransmission are often overlooked in model characterization (Smith, et al., 2012). Interestingly, a recent description of an aged mitochondrial protein kinase PINK1 (PTEN-induced kinase 1) knockout mouse model found olfactory deficits and gait abnormalities. These behavioral abnormalities were associated with serotonergic fiber loss in the absence of overt damage to the nigrostriatal dopamine system (Glasl, et al., 2012). Thus, the animal model we describe here and other recent models may reproduce certain features of serotonergic dysfunction in early stage PD.

Our findings are in agreement with many other mammalian genetic models that typically do not reproduce the major pathological features of end-stage PD. While this may be perceived as a weakness relative to acute neurotoxicant-based models, a recent review suggests that there is much to be learned form genetic models (Chesselet and Richter, 2011). Given that there was not overt nigral dopamine cell loss or detectable striatal dopamine depletion, it is unlikely that motor behavioral deficits would be quantifiable through commonly used assays, which are dependent on significant dopamine depletion. However, there are an array of specialized behavioral tests that can be used in bilateral rodent models to assess subtle autonomic and sensorimotor deficits (Fleming and Chesselet, 2006, Fleming, et al., 2012). Such tests should be utilized in future studies examining this model.

Current α-synuclein animal models with motor phenotypes typically have very high levels of α-synuclein expression (much higher than basal levels), show motor neuron degeneration, and little pathology in the nigrostriatal system (Giasson, et al., 2002, Lee, et al., 2002). These phenotypes are not found in the human disease, and while they are useful for many studies, they have limited use for understanding nigrostriatal degeneration or for neuroprotection studies. Because we are using a BAC, the concentration of α-synuclein and its distribution are more physiological. A major advantage of the model we have presented here is the ability to reproduce the accumulation and aggregation of α-synuclein in nigral dopamine neurons, which is a pathological hallmark of PD (Spillantini, et al., 1997), but generally not seen in other transgenic models. We also found that α-synuclein accumulation occurred in VTA. It is difficult to determine if this is representative of human E46K-PD. The most thorough pathological examination to date of human cases did not appear to examine this brain region (Zarranz, et al., 2004). Further, a recent mouse E46K transgenic model, showed primarily accumulation in the pons, without significant pathology in the substantia nigra (Emmer, et al., 2011). In our model, accumulation in other brain regions such as the striatum and cortex primarily appeared to be in neuronal processes.

The model we have described here involves the expression of a disease causing mutation in α-synuclein. To date, genetic approaches in the rat have been largely limited to surgical approaches (Welchko, et al., 2012). Additional BAC-transgenic rat models of PD are expected to be characterized in the near future. A recent report of an inducible leucine-rich repeat kinase-2 (LRRK2) rat model, while finding no major pathology in the nigrostriatal dopamine system, also suggests that transgenic rat PD lines may soon become much more prominent (Zhou, et al., 2011). The characterization of a model expressing non-mutant human α-synuclein would be an optimal control for the line described here. It would allow for mechanistic explorations on the pathological differences between non-mutant and mutant α-synuclein. Further, a model expressing non-mutant α-synuclein human may reproduce certain features of gene expansions that are responsible for some human PD cases.

Although the etiology of idiopathic PD is unknown, polygenic inheritance and environmental exposures are believed to play important roles in pathogenesis (Bekris, et al., 2010). In this regard, the animals described here are well-suited for future studies of crosses with other relevant genetic models and for studies investigating interactions with additional putative environmental factors.

Supplementary Material

Refer to Web version on PubMed Central for supplementary material.

Acknowledgments

This work was supported by the National Institutes of Health [ES019879 to J.R.C., 1RC1ES018058 to J.T.G. and C.L.] and the Michael J. Fox Foundation (to J.T.G. and C.L.).

Abbreviations

BAC	bacterial artificial chromosomal
DOPAC	3,4-dihydroxyphenylacetic acid
5-HIAA	5-hydroxyindole-3-aceitic acid
5-HT	serotonin
HVA	homovanillic acid
PD	Parkinson’s disease

References

1. Adams JR, van Netten H, Schulzer M, Mak E, McKenzie J, Strongosky A, Sossi V, Ruth TJ, Lee CS, Farrer M, Gasser T, Uitti RJ, Calne DB, Wszolek ZK, Stoessl AJ. PET in LRRK2 mutations: comparison to sporadic Parkinson's disease and evidence for presymptomatic compensation. Brain. 2005; 128:2777–2785. [PubMed: 16081470]
2. Bekris LM, Mata IF, Zabetian CP. The genetics of Parkinson disease. J Geriatr Psychiatry Neurol. 2010; 23:228–242. [PubMed: 20938043]
3. Betarbet R, Sherer TB, MacKenzie G, Garcia-Osuna M, Panov AV, Greenamyre JT. Chronic systemic pesticide exposure reproduces features of Parkinson's disease. Nat Neurosci. 2000; 3:1301–1306. [PubMed: 11100151]
4. Braak H, Del Tredici K, Rub U, de Vos RA, Jansen Steur EN, Braak E. Staging of brain pathology related to sporadic Parkinson's disease. Neurobiol Aging. 2003; 24:197–211. [PubMed: 12498954]
5. Braak H, Ghebremedhin E, Rub U, Bratzke H, Del Tredici K. Stages in the development of Parkinson's disease-related pathology. Cell Tissue Res. 2004; 318:121–134. [PubMed: 15338272]
6. Cannon JR, Greenamyre JT. Neurotoxic in vivo models of Parkinson's disease recent advances. Prog Brain Res. 2010; 184:17–33. [PubMed: 20887868]
7. Cannon JR, Sew T, Montero L, Burton EA, Greenamyre JT. Pseudotype-dependent lentiviral transduction of astrocytes or neurons in the rat substantia nigra. Exp Neurol. 2011; 228:41–52. [PubMed: 21056560]
8. Cannon JR, Tapias V, Na HM, Honick AS, Drolet RE, Greenamyre JT. A highly reproducible rotenone model of Parkinson's disease. Neurobiol Dis. 2009; 34:279–290. [PubMed: 19385059]
9. Chandran JS, Lin X, Zapata A, Hoke A, Shimoji M, Moore SO, Galloway MP, Laird FM, Wong PC, Price DL, Bailey KR, Crawley JN, Shippenberg T, Cai H. Progressive behavioral deficits in DJ-1-deficient mice are associated with normal nigrostriatal function. Neurobiol Dis. 2008; 29:505–514. [PubMed: 18187333]
10. Chesselet MF, Richter F. Modelling of Parkinson's disease in mice. Lancet Neurol. 2011; 10:1108–1118. [PubMed: 22094131]
11. Choi W, Zibaee S, Jakes R, Serpell LC, Davletov B, Crowther RA, Goedert M. Mutation E46K increases phospholipid binding and assembly into filaments of human alpha-synuclein. FEBS Lett. 2004; 576:363–368. [PubMed: 15498564]
12. Emmer KL, Waxman EA, Covy JP, Giasson BI. E46K human alpha-synuclein transgenic mice develop Lewy-like and tau pathology associated with age-dependent, detrimental motor impairment. J Biol Chem. 2011; 286:35104–35118. [PubMed: 21846727]
13. Filipiak WE, Saunders TL. Advances in transgenic rat production. Transgenic Res. 2006; 15:673–686. [PubMed: 17009096]
14. Fleming SM, Chesselet MF. Behavioral phenotypes and pharmacology in genetic mouse models of Parkinsonism. Behav Pharmacol. 2006; 17:383–391. [PubMed: 16940759]
15. Fleming SM, Schallert T, Ciucci MR. Cranial and related sensorimotor impairments in rodent models of Parkinson's disease. Behav Brain Res. 2012; 231:317–322. [PubMed: 22394540]
16. Forno LS. Neuropathology of Parkinson's disease. J Neuropathol Exp Neurol. 1996; 55:259–272. [PubMed: 8786384]

17. Giasson BI, Duda JE, Quinn SM, Zhang B, Trojanowski JQ, Lee VM. Neuronal alpha-synucleinopathy with severe movement disorder in mice expressing A53T human alpha-synuclein. Neuron. 2002; 34:521–533. [PubMed: 12062037]

18. Glasl L, Kloos K, Giesert F, Roethig A, Di Benedetto B, Kuhn R, Zhang J, Hafen U, Zerle J, Hofmann A, de Angelis MH, Winklhofer KF, Holter SM, Vogt Weisenhorn DM, Wurst W. Pink1-deficiency in mice impairs gait, olfaction and serotonergic innervation of the olfactory bulb. Exp Neurol. 2012; 235:214–227. [PubMed: 22265660]

19. Goerendt IK, Messa C, Lawrence AD, Grasby PM, Piccini P, Brooks DJ. Dopamine release during sequential finger movements in health and Parkinson's disease: a PET study. Brain. 2003; 126:312–325. [PubMed: 12538400]

20. Goldberg MS, Fleming SM, Palacino JJ, Cepeda C, Lam HA, Bhatnagar A, Meloni EG, Wu N, Ackerson LC, Klapstein GJ, Gajendiran M, Roth BL, Chesselet MF, Maidment NT, Levine MS, Shen J. Parkin-deficient mice exhibit nigrostriatal deficits but not loss of dopaminergic neurons. J Biol Chem. 2003; 278:43628–43635. [PubMed: 12930822]

21. Goldberg MS, Pisani A, Haburcak M, Vortherms TA, Kitada T, Costa C, Tong Y, Martella G, Tscherter A, Martins A, Bernardi G, Roth BL, Pothos EN, Calabresi P, Shen J. Nigrostriatal dopaminergic deficits and hypokinesia caused by inactivation of the familial Parkinsonism-linked gene DJ-1. Neuron. 2005; 45:489–496. [PubMed: 15721235]

22. Gong S, Yang XW, Li C, Heintz N. Highly efficient modification of bacterial artificial chromosomes (BACs) using novel shuttle vectors containing the R6Kgamma origin of replication. Genome Res. 2002; 12:1992–1998. [PubMed: 12466304]

23. Guttman M, Boileau I, Warsh J, Saint-Cyr JA, Ginovart N, McCluskey T, Houle S, Wilson A, Mundo E, Rusjan P, Meyer J, Kish SJ. Brain serotonin transporter binding in non-depressed patients with Parkinson's disease. Eur J Neurol. 2007; 14:523–528. [PubMed: 17437611]

24. Itier JM, Ibanez P, Mena MA, Abbas N, Cohen-Salmon C, Bohme GA, Laville M, Pratt J, Corti O, Pradier L, Ret G, Joubert C, Periquet M, Araujo F, Negroni J, Casarejos MJ, Canals S, Solano R, Serrano A, Gallego E, Sanchez M, Denefle P, Benavides J, Tremp G, Rooney TA, Brice A, Garcia de Yebenes J. Parkin gene inactivation alters behaviour and dopamine neurotransmission in the mouse. Hum Mol Genet. 2003; 12:2277–2291. [PubMed: 12915482]

25. Kitada T, Pisani A, Karouani M, Haburcak M, Martella G, Tscherter A, Platania P, Wu B, Pothos EN, Shen J. Impaired dopamine release and synaptic plasticity in the striatum of parkin−/− mice. J Neurochem. 2009; 110:613–621. [PubMed: 19457102]

26. Kitada T, Pisani A, Porter DR, Yamaguchi H, Tscherter A, Martella G, Bonsi P, Zhang C, Pothos EN, Shen J. Impaired dopamine release and synaptic plasticity in the striatum of PINK1-deficient mice. Proc Natl Acad Sci U S A. 2007; 104:11441–11446. [PubMed: 17563363]

27. Lee MK, Stirling W, Xu Y, Xu X, Qui D, Mandir AS, Dawson TM, Copeland NG, Jenkins NA, Price DL. Human alpha-synuclein-harboring familial Parkinson's disease-linked Ala-53 --> Thr mutation causes neurodegenerative disease with alpha-synuclein aggregation in transgenic mice. Proc Natl Acad Sci U S A. 2002; 99:8968–8973. [PubMed: 12084935]

28. Litvan I, Bhatia KP, Burn DJ, Goetz CG, Lang AE, McKeith I, Quinn N, Sethi KD, Shults C, Wenning GK. Movement Disorders Society Scientific Issues Committee report: SIC Task Force appraisal of clinical diagnostic criteria for Parkinsonian disorders. Mov Disord. 2003; 18:467–486. [PubMed: 12722160]

29. Lowry OH, Rosebrough NJ, Farr AL, Randall RJ. Protein measurement with the Folin phenol reagent. J Biol Chem. 1951; 193:265–275. [PubMed: 14907713]

30. Manning-Bog AB, Caudle WM, Perez XA, Reaney SH, Paletzki R, Isla MZ, Chou VP, McCormack AL, Miller GW, Langston JW, Gerfen CR, Dimonte DA. Increased vulnerability of nigrostriatal terminals in DJ-1-deficient mice is mediated by the dopamine transporter. Neurobiol Dis. 2007; 27:141–150. [PubMed: 17560790]

31. Masliah E, Rockenstein E, Veinbergs I, Mallory M, Hashimoto M, Takeda A, Sagara Y, Sisk A, Mucke L. Dopaminergic loss and inclusion body formation in alpha-synuclein mice: implications for neurodegenerative disorders. Science. 2000; 287:1265–1269. [PubMed: 10678833]

32. McLean JR, Hallett PJ, Cooper O, Stanley M, Isacson O. Transcript expression levels of full-length alpha-synuclein and its three alternatively spliced variants in Parkinson's disease brain

regions and in a transgenic mouse model of alpha-synuclein overexpression. Mol Cell Neurosci. 2012; 49:230–239. [PubMed: 22155155]

33. Metcalf WW, Jiang W, Daniels LL, Kim SK, Haldimann A, Wanner BL. Conditionally replicative and conjugative plasmids carrying lacZ alpha for cloning, mutagenesis, and allele replacement in bacteria. Plasmid. 1996; 35:1–13. [PubMed: 8693022]
34. Nandhagopal R, Mak E, Schulzer M, McKenzie J, McCormick S, Sossi V, Ruth TJ, Strongosky A, Farrer MJ, Wszolek ZK, Stoessl AJ. Progression of dopaminergic dysfunction in a LRRK2 kindred: a multitracer PET study. Neurology. 2008; 71:1790–1795. [PubMed: 19029519]
35. Perez FA, Curtis WR, Palmiter RD. Parkin-deficient mice are not more sensitive to 6-hydroxydopamine or methamphetamine neurotoxicity. BMC Neurosci. 2005; 6:71. [PubMed: 16375772]
36. Politis M, Loane C. Serotonergic dysfunction in Parkinson's disease and its relevance to disability. Scientific World Journal. 2011; 11:1726–1734. [PubMed: 22125431]
37. Polymeropoulos MH, Lavedan C, Leroy E, Ide SE, Dehejia A, Dutra A, Pike B, Root H, Rubenstein J, Boyer R, Stenroos ES, Chandrasekharappa S, Athanassiadou A, Papapetropoulos T, Johnson WG, Lazzarini AM, Duvoisin RC, Di Iorio G, Golbe LI, Nussbaum RL. Mutation in the alpha-synuclein gene identified in families with Parkinson's disease. Science. 1997; 276:2045–2047. [PubMed: 9197268]
38. Richfield EK, Thiruchelvam MJ, Cory-Slechta DA, Wuertzer C, Gainetdinov RR, Caron MG, Di Monte DA, Federoff HJ. Behavioral and neurochemical effects of wild-type and mutated human alpha-synuclein in transgenic mice. Exp Neurol. 2002; 175:35–48. [PubMed: 12009758]
39. Schwarting RK, Huston JP. Unilateral 6-hydroxydopamine lesions of meso-striatal dopamine neurons and their physiological sequelae. Prog Neurobiol. 1996; 49:215–266. [PubMed: 8878304]
40. Shizuya H, Birren B, Kim UJ, Mancino V, Slepak T, Tachiiri Y, Simon M. Cloning and stable maintenance of 300-kilobase-pair fragments of human DNA in Escherichia coli using an F-factor-based vector. Proc Natl Acad Sci U S A. 1992; 89:8794–8797. [PubMed: 1528894]
41. Singleton AB, Farrer M, Johnson J, Singleton A, Hague S, Kachergus J, Hulihan M, Peuralinna T, Dutra A, Nussbaum R, Lincoln S, Crawley A, Hanson M, Maraganore D, Adler C, Cookson MR, Muenter M, Baptista M, Miller D, Blancato J, Hardy J, Gwinn-Hardy K. alpha-Synuclein locus triplication causes Parkinson's disease. Science. 2003; 302:841. [PubMed: 14593171]
42. Smith GA, Isacson O, Dunnett SB. The search for genetic mouse models of prodromal Parkinson's disease. Exp Neurol. 2012; 237:267–273. [PubMed: 22819262]
43. Spillantini MG, Schmidt ML, Lee VM, Trojanowski JQ, Jakes R, Goedert M. Alpha-synuclein in Lewy bodies. Nature. 1997; 388:839–840. [PubMed: 9278044]
44. Strafella AP, Ko JH, Grant J, Fraraccio M, Monchi O. Corticostriatal functional interactions in Parkinson's disease: a rTMS/[11C]raclopride PET study. Eur J Neurosci. 2005; 22:2946–2952. [PubMed: 16324129]
45. Tanner CM, Kamel F, Ross GW, Hoppin JA, Goldman SM, Korell M, Marras C, Bhudhikanok GS, Kasten M, Chade AR, Comyns K, Richards MB, Meng C, Priestley B, Fernandez HH, Cambi F, Umbach DM, Blair A, Sandler DP, Langston JW. Rotenone, paraquat, and Parkinson's disease. Environ Health Perspect. 2011; 119:866–872. [PubMed: 21269927]
46. Tapias V, Cannon JR, Greenamyre JT. Melatonin treatment potentiates neurodegeneration in a rat rotenone Parkinson's disease model. J Neurosci Res. 2010; 88:420–427. [PubMed: 19681169]
47. Von Coelln R, Thomas B, Savitt JM, Lim KL, Sasaki M, Hess EJ, Dawson VL, Dawson TM. Loss of locus coeruleus neurons and reduced startle in parkin null mice. Proc Natl Acad Sci U S A. 2004; 101:10744–10749. [PubMed: 15249681]
48. Welchko RM, Leveque XT, Dunbar GL. Genetic rat models of Parkinson's disease. Parkinsons Dis. 2012; 2012 128356.
49. Whishaw, IQ.; Kolb, B. The behavior of the laboratory rat: a handbook with tests. Oxford: Oxford University Press; 2004.
50. Yamaguchi H, Shen J. Absence of dopaminergic neuronal degeneration and oxidative damage in aged DJ-1-deficient mice. Mol Neurodegener. 2007; 2:10. [PubMed: 17535435]
51. Yang XW, Gong S. An overview on the generation of BAC transgenic mice for neuroscience research. Curr Protoc Neurosci. 2005; Chapter 5(Unit 5):20. [PubMed: 18428622]

52. Yavich L, Oksman M, Tanila H, Kerokoski P, Hiltunen M, van Groen T, Puolivali J, Mannisto PT, Garcia-Horsman A, MacDonald E, Beyreuther K, Hartmann T, Jakala P. Locomotor activity and evoked dopamine release are reduced in mice overexpressing A30P-mutated human alpha-synuclein. Neurobiol Dis. 2005; 20:303–313. [PubMed: 16242637]

53. Zarranz JJ, Alegre J, Gomez-Esteban JC, Lezcano E, Ros R, Ampuero I, Vidal L, Hoenicka J, Rodriguez O, Atares B, Llorens V, Gomez Tortosa E, del Ser T, Munoz DG, de Yebenes JG. The new mutation, E46K, of alpha-synuclein causes Parkinson and Lewy body dementia. Ann Neurol. 2004; 55:164–173. [PubMed: 14755719]

54. Zhou H, Huang C, Tong J, Hong WC, Liu YJ, Xia XG. Temporal expression of mutant LRRK2 in adult rats impairs dopamine reuptake. Int J Biol Sci. 2011; 7:753–761. [PubMed: 21698001]

Highlights

- We created and characterized a new transgenic rat model of Parkinson's disease
- Expression of E46K α-synuclein does not cause dopamine depletion or cell loss
- E46K α-synuclein rats exhibit features of preclinical Parkinson's disease
- These rats exhibit enhanced sensitivity to rotenone

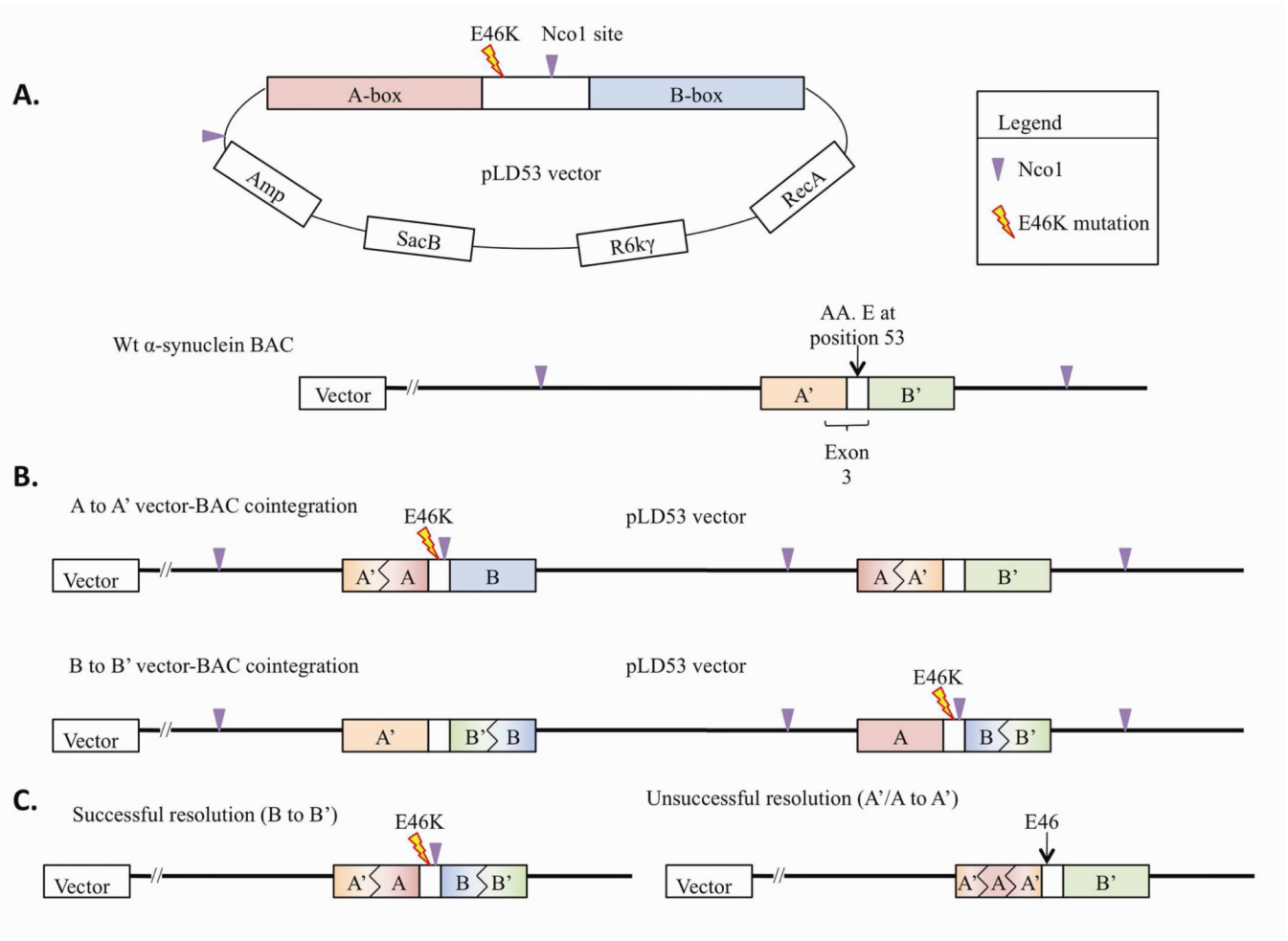

Figure 1.

Schematic of α-synuclein BAC modification to insert E46K point mutation. (A) Depiction of the pLD53 vector with the E46K mutation surrounding homology arms. Created and natural Nco1 sites are depicted. The unmodified BAC shows the natural E46 site, as well as natural Nco1 sites. (B) These depictions show the two possibilities of vector-BAC cointegration: either via homologous recombination of the A-box homology arm, or via homologous recombination of the B-box homology arm. (C) The two possible resolution outcomes are either via A-box or B-box homologous recombination. As the pLD53 vector cointegrated in the A-box homology arm, successful resolution can only occur via B-box homologous recombination. Two possible outcomes are depicted: A-box resolution to return the BAC to its original state, or B-box resolution to create an E46K mutated BAC.

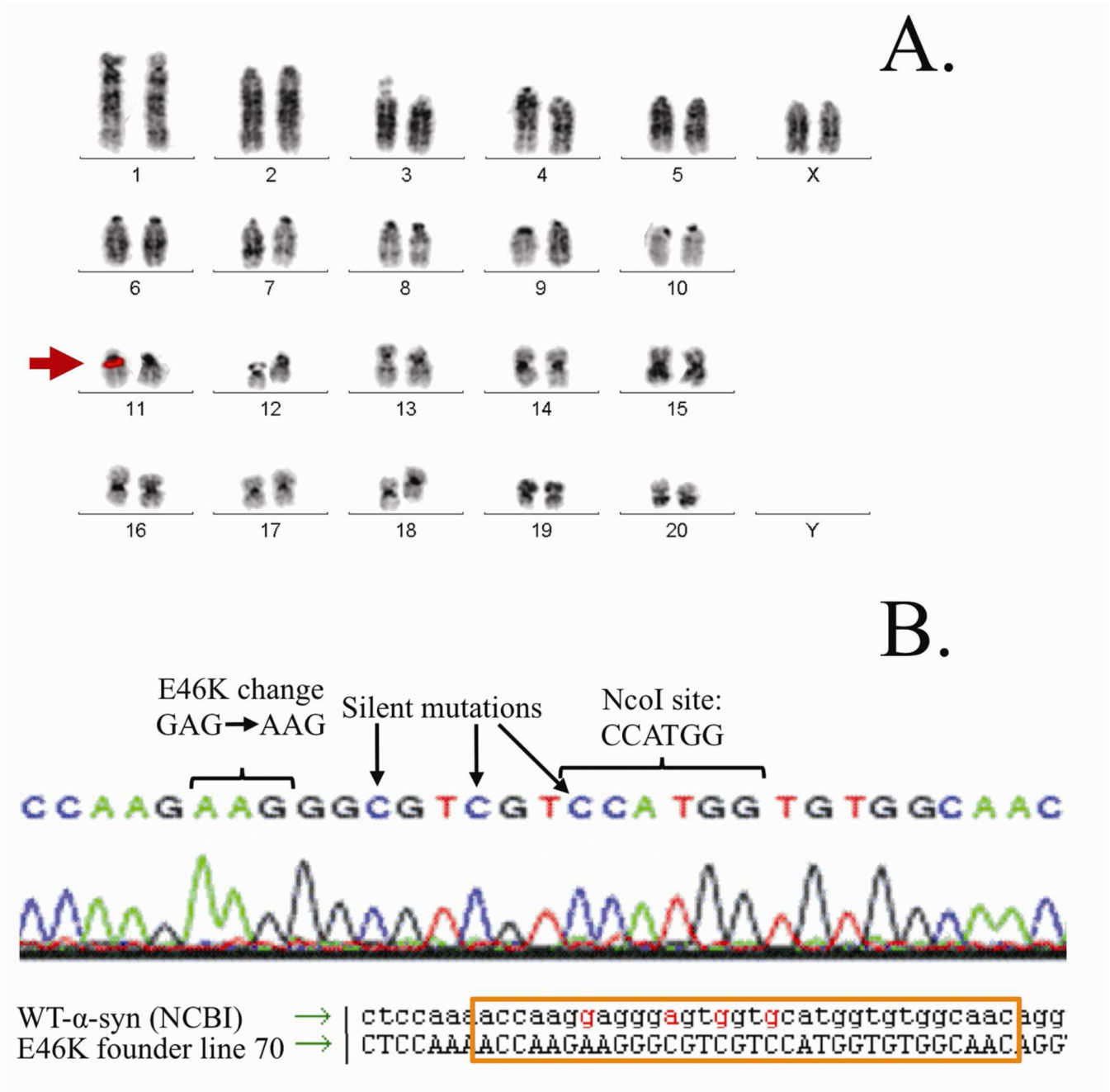

Figure 2.
E46K BAC chromosome insertion site and sequence. (A) FISH hybridization of Founder 70 identified chromosome 11q11 as the single insertion site of the human E46K α-synuclein transgene. (B) Sequencing of Founder 70 revealed the intended E to K point mutation at position 46 (GAG to AAG). Three additional engineered silent mutations were also present: one mutation created an NcoI site for easy mutant gene identification, and two extra mutations to sufficiently differentiate the sequence so that only surrounding regions (the 'A' box and 'B' box) underwent homologous recombination.

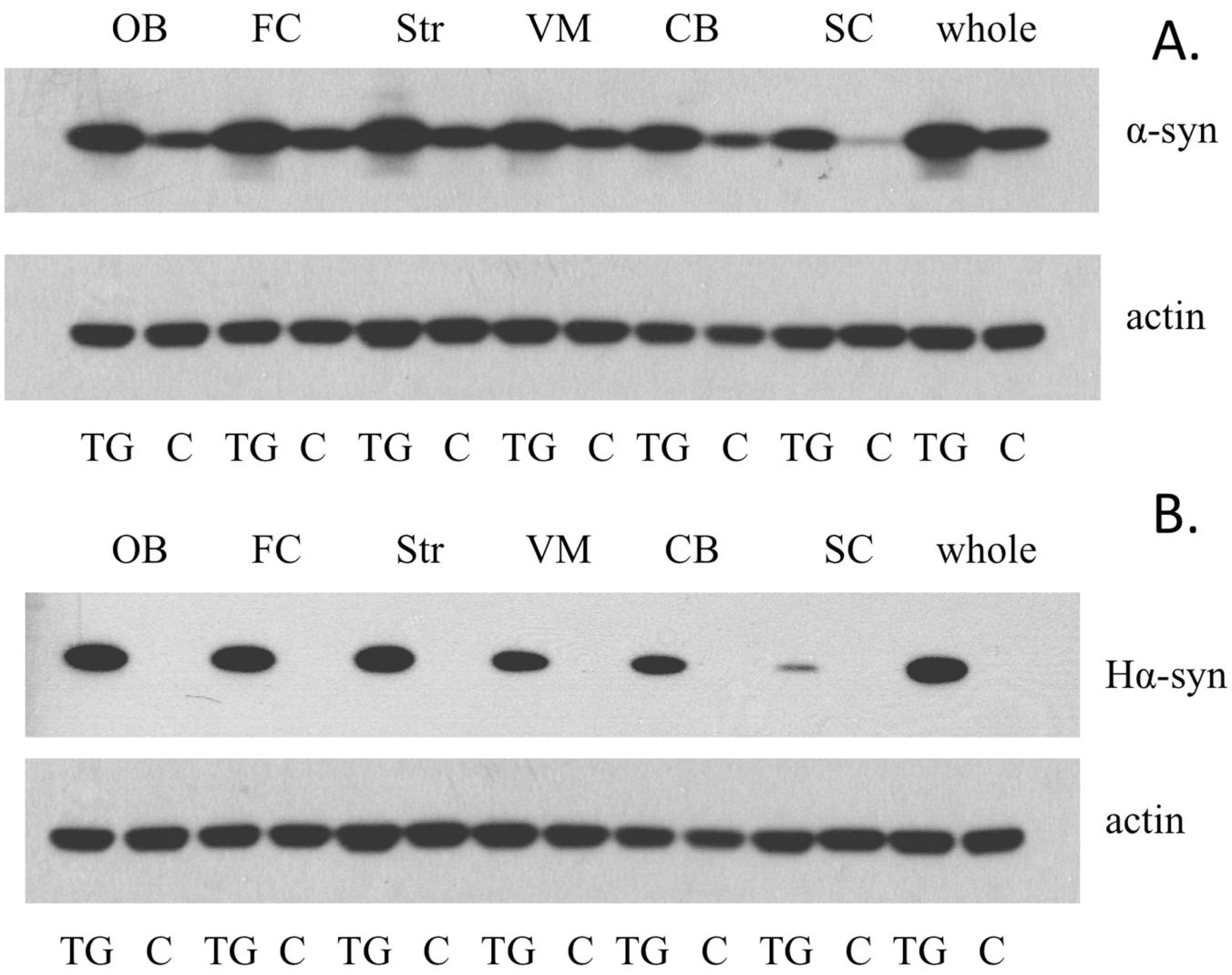

Figure 3.

α-Synuclein regional expression demonstrates a more accurate spatio-temporal expression of E46K transgene. (A) Expression of total α-synuclein from transgenic (TG) and endogenous *wild-type* (WT; littermate controls) animals. (B) E46K expression of human-specific α-synuclein. Abbreviations: OB = olfactory bulb, FC = frontal cortex, Str = striatum, VM = ventral midbrain, CB = cerebellum, SC = spinal cord, whole = whole brain.

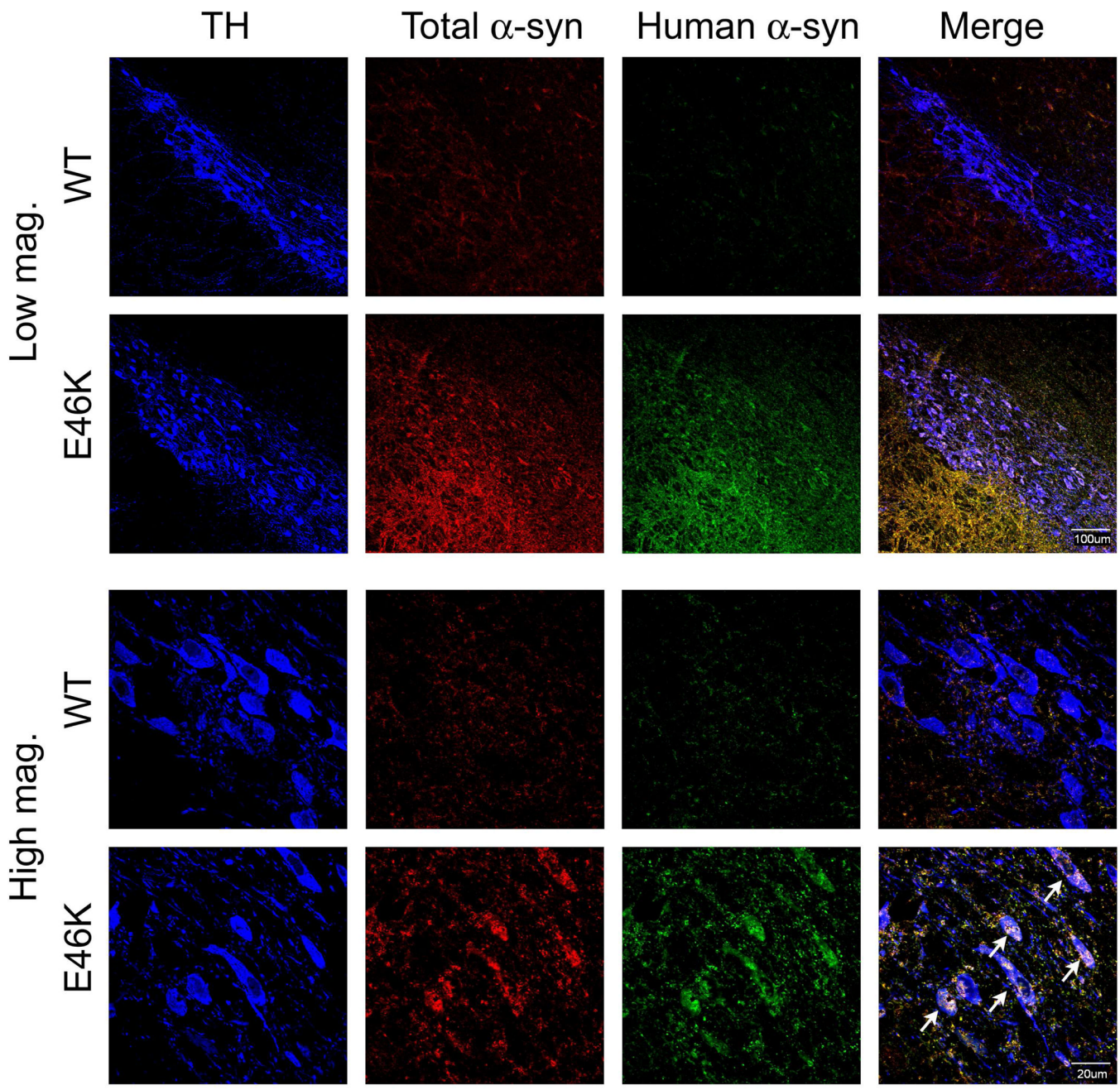

Figure 4.

α-Synuclein accumulation and aggregation in the substantia nigra. Animals (12-month old) expressing E46K-mutated α-synuclein exhibit overt accumulation and aggregation of α-synuclein. Low magnification images show diffuse accumulation of both total and aggregated human α-synuclein. High magnification images show both neuropil (likely in processes) and intracellular accumulation and aggregation in nigral dopamine neurons (tyrosine hydroxylase +, TH). The morphology of E46K neurons is also altered compared to *wild-type* (WT; littermate controls), where the cell membrane appears to be undergoing fragmentation (indicated by arrows).

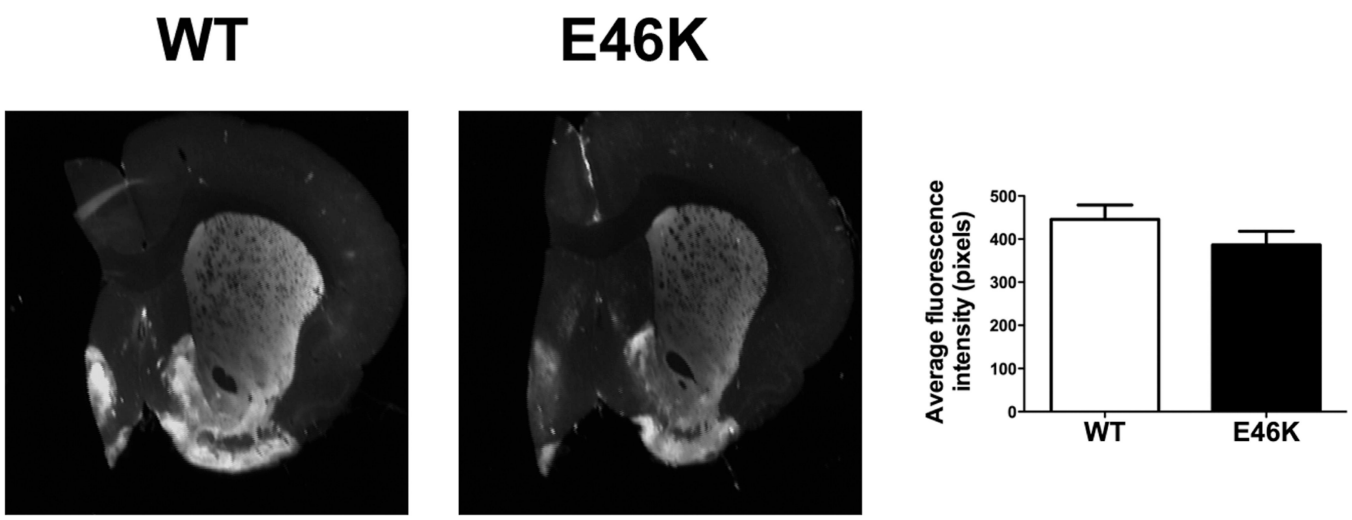

Figure 5.

Striatal dopamine terminal density is not significantly reduced in 12-month old transgenic (TG) rats. The reduction in striatal tyrosine hydroxylase immunofluorescence in E46K α-synuclein rats versus *wild-type* (WT; littermate controls) did not reach significance. $n = 10$/group.

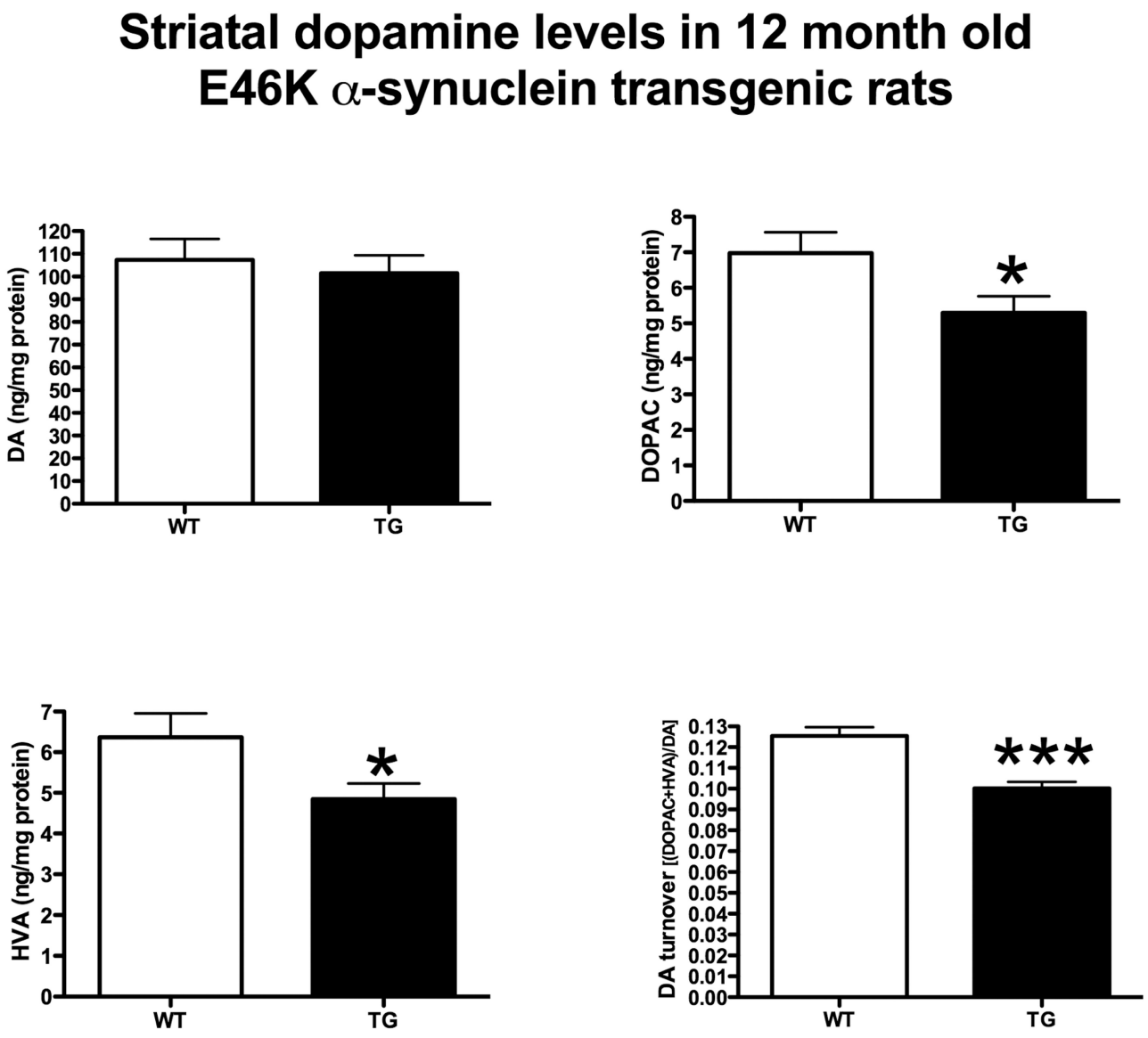

Figure 6.

Striatal dopamine (DA) and dopamine metabolite levels in 12 month-old rats. Transgenic (TG) rats expressing E46K-mutated α-synuclein did not exhibit differences in basal dopamine levels compared to *wild-type* (WT; littermate controls). However, TG rats exhibited decreased DA metabolite levels. 3,4-Dihydroxyphenylacetic acid (DOPAC) and homovanillic acid (HVA) were both significantly reduced in TG rats. DA turnover [(DOPAC+HVA)/DA] was also significantly reduced. *p<0.05, ***p<0.001, Student's t-test. n = 10/group.

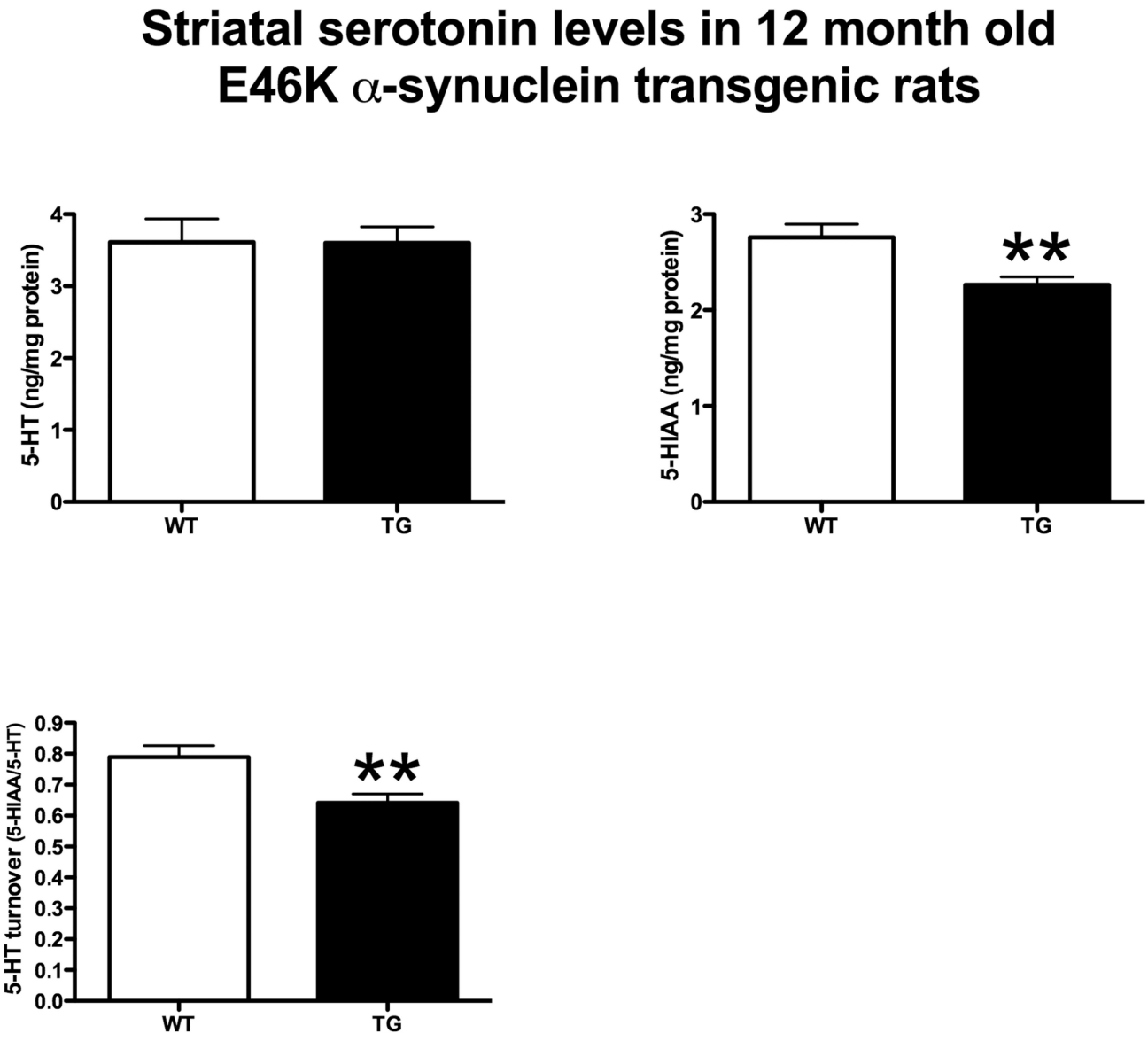

Figure 7.

Striatal serotonin (5-HT) and serotonin metabolite levels in 12 month-old rats. Transgenic (TG) rats expressing E46K mutated α-synuclein did not exhibit differences in basal serotonin levels compared to *wild-type* (WT; littermate controls). However, TG rats exhibited decreased 5-HT metabolite levels. 5-Hydroxyindole-3-acetic acid (5-HIAA) was significantly reduced in TG rats. 5-HT turnover (5-HIAA/5-HT) was also significantly reduced. ** $p<0.01$, Student's *t*-test. $n = 10$/group.

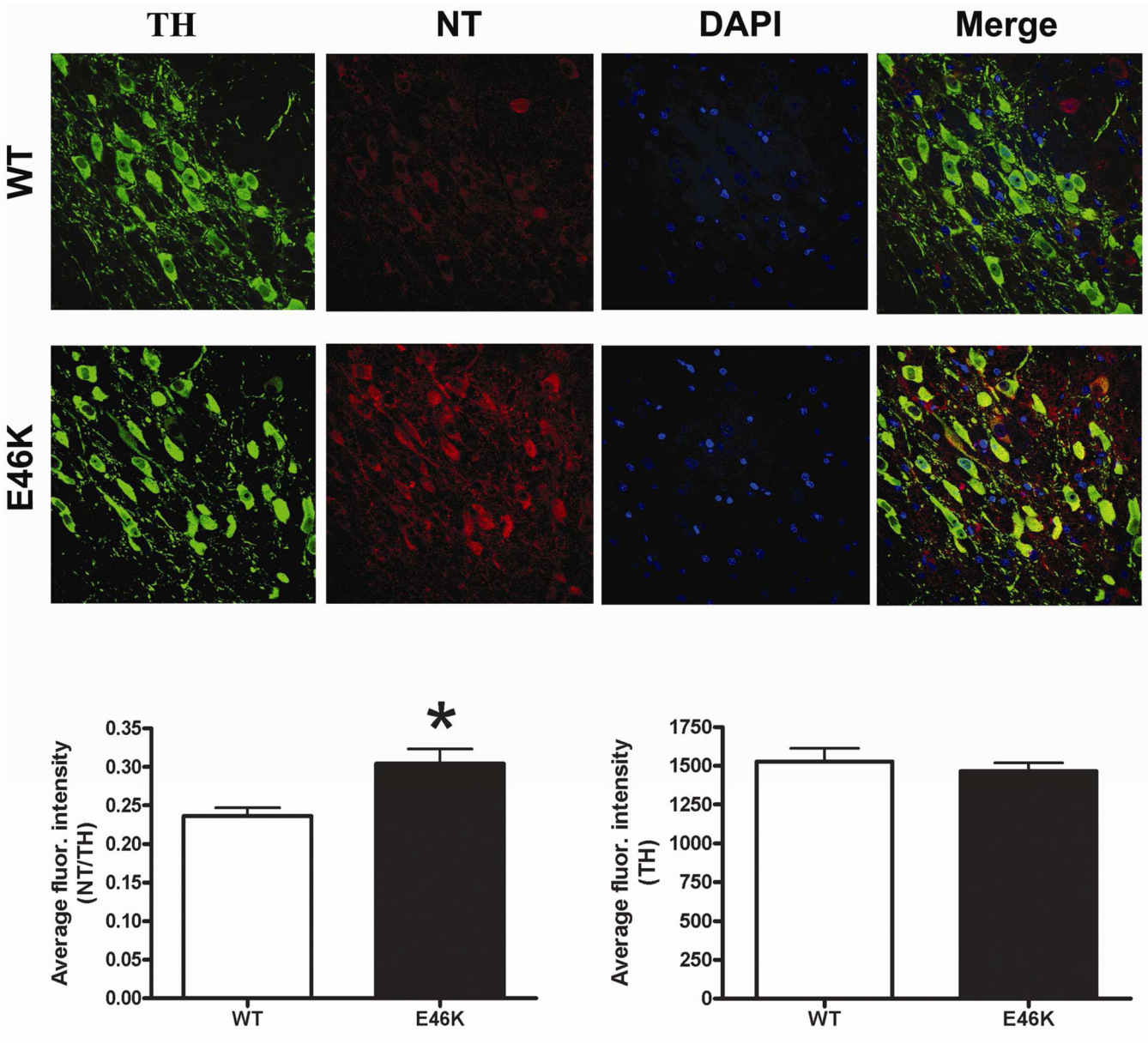

Figure 8.

Evidence of oxidative stress in animals expressing E46K mutated α-synuclein. Immunofluorescence for nitrotyrosine (NT) was quantified in individual dopaminergic neurons (tyrosine hydroxylase +, TH) of the substantia nigra. NT levels were expressed relative to TH. Transgenic (TG) rats (12 months old) exhibited significantly elevated NT levels in nigral dopamine neurons compared to *wild-type* (WT; littermate controls). Levels of TH alone were not different between groups. n = 6/group, >150 cells/animal analyzed. *p<0.05, Student's t-test.

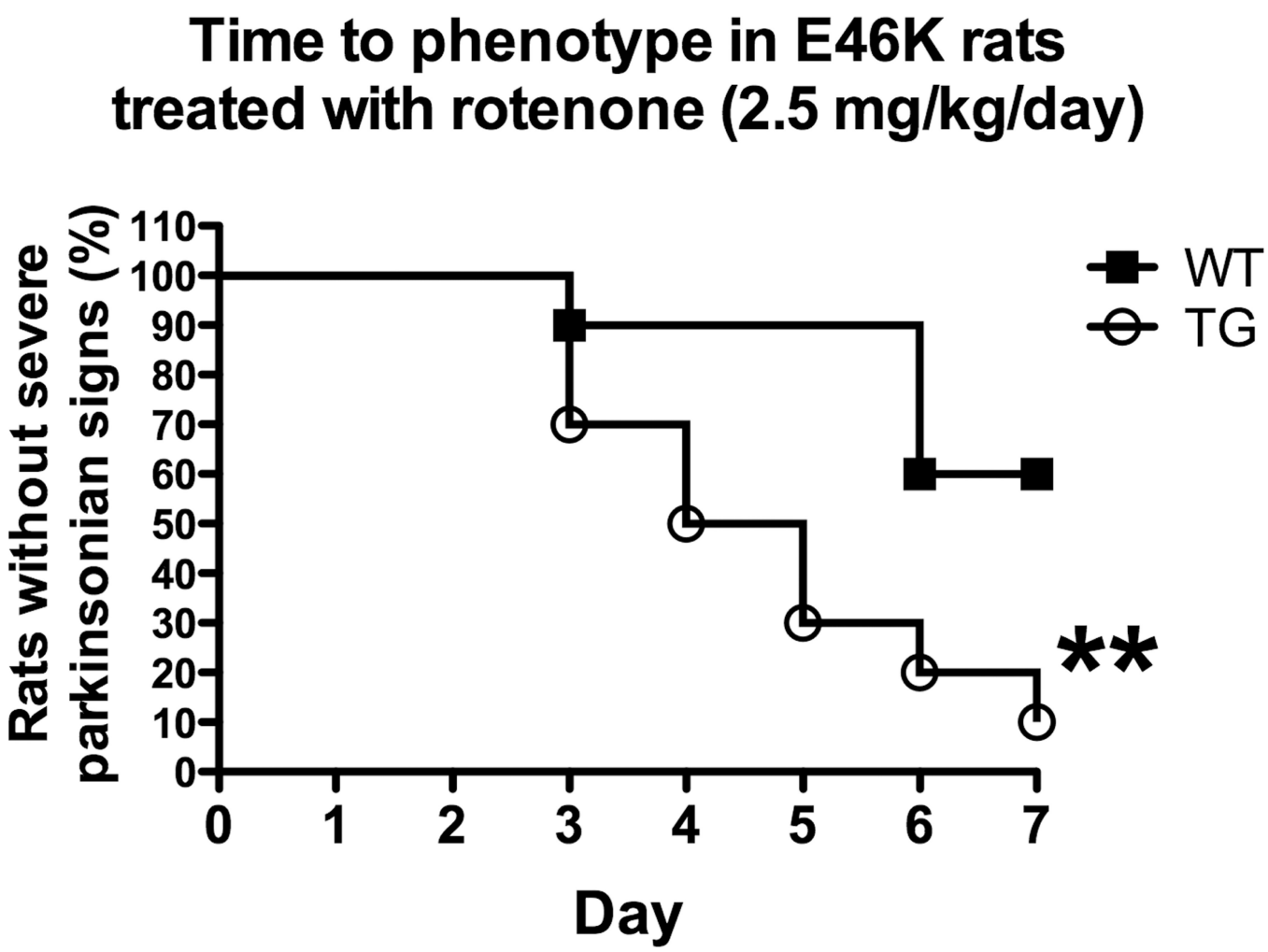

Figure 9.

Animals expressing E46K-mutated α-synuclein (6 months old) exhibit heightened sensitivity to rotenone. At a rotenone dose (2.5 mg/kg/day) that typically induces few symptoms in *wild-type* (WT; littermate controls) rats, those expressing E46K-mutated α-synuclein (squares) exhibited earlier onset of symptoms and the development of a severe PD phenotype (severe bradykinesia, postural instability, and rigidity) in a much higher percentage of animals. $n = 10$/group. $^{**}p<0.01$, Log-rank test.

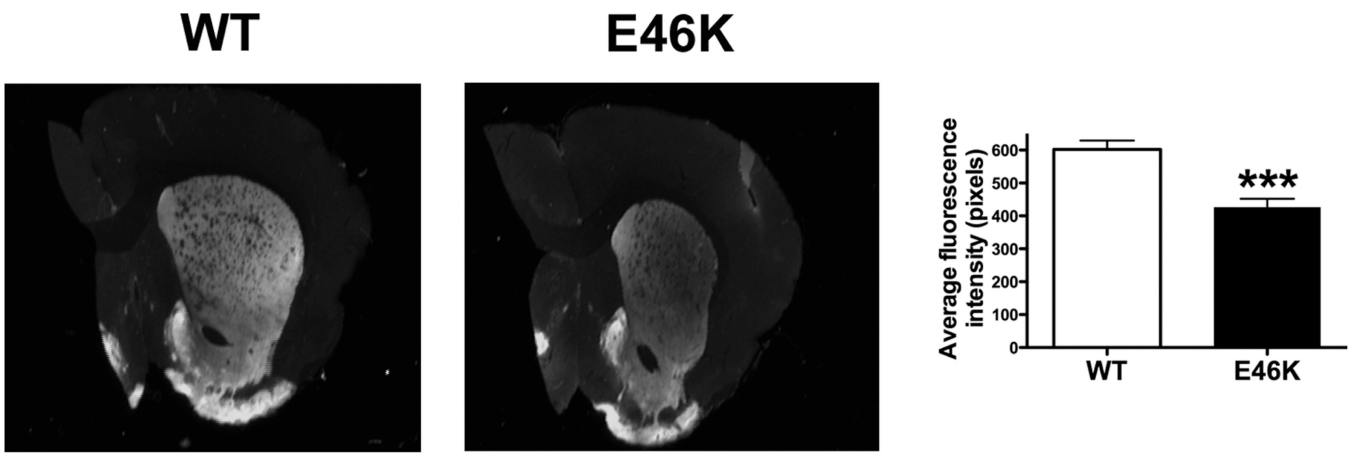

Figure 10.

Potentiation of striatal dopamine terminal loss in 6 month old transgenic (TG) rats exposed to low-dose rotenone. Animals expressing E46K-mutated α-synuclein exhibit decreased striatal tyrosine hydroxylase immunofluorescence at subthreshold rotenone exposure (2.5 mg/kg/day). A typical striatal lesion is observed in E46K animals, overt lesions are not typically present *wild-type* (WT; littermate controls) animals at this rotenone dose. $n = 10$/group. ***$p<0.001$, Student's *t*-test.

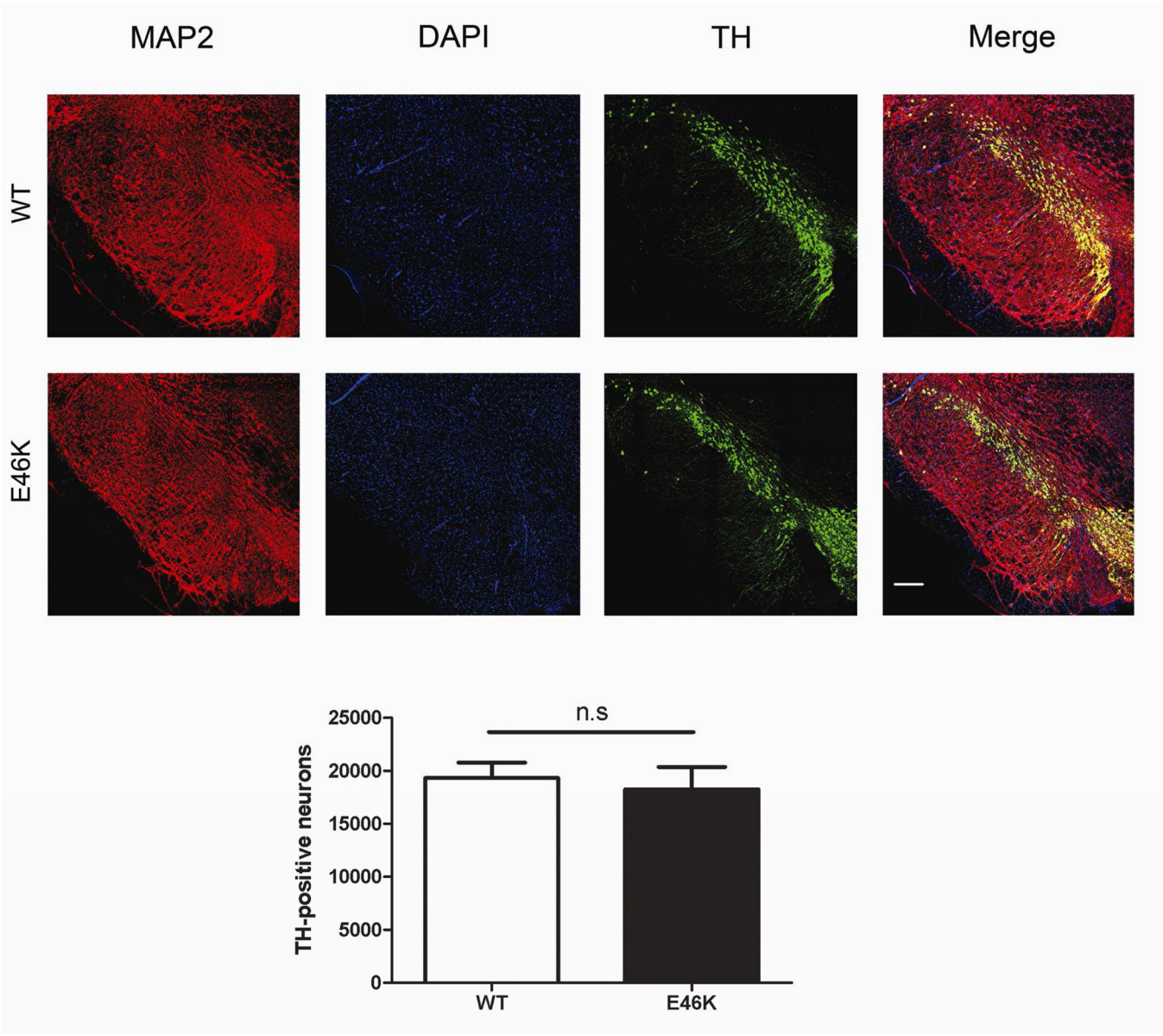

Figure 11.
Potentiation does not extend to the level of nigral dopamine cell bodies in 6 month old transgenic (TG) rats treated with low-dose rotenone. Cell counts of dopamine neurons in the substantia nigra did not show differences between *wild-type* (WT; littermate controls) and TG rats, indicating that the E46K-mediated potentiation, occurred primarily at the level of the dopamine terminals. $n = 6$/group.

Table 1

Primers used to design and validate transgenic rats expressing E46K mutated α-synuclein.

1.1. Primers designed to create the AB box. Capitalized "Outside primers" indicate attached base pairs to create restriction sites. "Inside primers" indicate the total size of the PCR sequence.			
Outside primers	A Box Forward	GGCGCGCCgatggtctcgatctcctgac	
	B Box Reverse	TTAATTAAcactctcatcctcatcttcctc	
Inside primers	E46K A Box Reverse	ccatggacgacgcccttcttggttttggagcctac	596bp
	E46K B Box Forward	aagaagggcgtcgtccatggtgtggcaacaggtaagc	700bp

1.2. Primers designed to sequence the six α-synuclein exons and their surrounding intronic regions. The size of the PCR sequence is also given.			
Exon	**5' Forward primer 3'**	**5' Reverse primer 3'**	**Size**
1	gagatagggacgaggagcac	ggacgaaagccaggtcaagtc	740bp
2	gccaagatggatgggagatg	tcacaggggcatatcaaagtc	778bp
3*	gagttcatgccattcttctg	cttttgcttcaccacatctgc	1508bp
4	gttgtgggcacctgtaatcc	atttgcatggcatttatctgg	937bp
5	aaatgatccacctgcctcag	tcttcatcttcctcctcctc	707bp
6	taactctgactactactactg	ccacaaaatccacagcacac	492bp

(*) indicates that this primer sequence pair surrounds the region containing the mutated exon.